Chapter 13

Practical Use of Multispectral Techniques for the Detection of Pathologies in Constructions

L.J. Sánchez-Aparicio, S. Del Pozo, P. Rodríguez-Gonzálvez, J. Herrero-Pascual, A. Muñoz-Nieto and D. González-Aguilera
Department of Cartographic and Land Engineering, High School of Ávila, University of Salamanca, Ávila, Spain

D. Hernández-López
Regional Development Institute-IDR, University of Castilla-La Mancha, Albacete, Spain

Abstract

Our approach to multispectral remote sensing assessment of constructive pathologies has been organized in two different parts. The first one (Chapter 7) dealt with equipment and methods. The second one, developed in this chapter, will be related to the application to real cases, encompassing relevant aspects such as: data acquisition (sensor type choice and field works planning), processing (filtering and segmentation), sensor registration, true orthophoto generation, orthophoto classifications (through supervised and unsupervised techniques) and the qualitative and quantitative analysis of results (by means of confusion matrix, spectral separability, overall accuracy, reliability and agreement of informational classes). Based on these premises three case studies have been addressed. On the one hand, two historical stone masonry constructions and on the other hand one modern reinforced concrete construction. These three case studies will be used as examples of best practices in multispectral dataset management and processing, and will serve to evaluate the flexibility of the methodology proposed for detecting and classifying accurately a wide range of constructive pathologies.

13.1 Introduction

Chapter 7 addressed, from a theoretical point of view, a study of instrumentation and methods to process multispectral datasets of different building elements. This chapter will describe and analyze a selected group of experiences resulting from the application of such methodologies in two of the most significant civil engineering fields such as cultural heritage constructions and buildings and civil infrastructures.

Safeguarding and enhancement of the built heritage can be considered a fundamental feature for modern developed societies. Sometimes by its own intrinsic value, and also for its artistic or cultural value, preservation of these types of constructions becomes extremely important. Due to their unique nature or their fragility it is necessary to know thoroughly their geometric and structural characteristics and, where appropriate,

provide information to establish intervention plans based on a comprehensive diagnosis and assessment of their pathologies. Experience in conservation and restoration projects highlights the need to use non-destructive techniques to acquire required datasets. This fact restricts the use of some techniques and sensors.

The exposure to chemically aggressive environments, moisture or biological organisms produces deteriorations that usually worsen over time. This situation is especially pronounced in constructions and old buildings. However, modern buildings and civil infrastructures that use different materials and construction techniques also suffer different types of deterioration.

The case studies submitted below have been selected within a broader set of experiences developed by the research group TIDOP (Armesto-González et al. 2010, Crespo et al. 2010, Del Pozo et al. 2015, González-Jorge et al. 2012, Rodríguez-Gonzálvez et al. 2013), which belongs to the University of Salamanca (http://tidop.usal.es), in order to offer a wide casuistry applying multispectral data in diagnosis and assessment of pathologies in constructions.

Following a common structure, the next items will be addressed in each case study:

- Description and building materials: after a brief introduction of the case study, a broad description of materials and construction technics will be done.
- Pathological assessment: as a result of the constructive elements analyzed, a brief description of the expected pathologies will be assessed.
- Sensors and methods: under these paragraphs the characteristics of the used sensors and the methodology applied in the data process will be explained.
- Experimental results: these paragraphs will show, by means of graphics and statistical analysis, an objective assessment of the followed methodology. The main issues to be considered in the analysis of multispectral images are: (i) Separability; (ii) Cohen's Kappa coefficient; (iii) Overall accuracy; and (iv) Comparative study between supervised and non-supervised classifications.

The following table (Table 13.1) synthesizes the technical specifications of the sensors that have been used. The next figure (Fig. 13.1) shows, schematically, the workflow applied to data processing, which is common for most cases.

To complete this chapter, a best practices guide, derived from case studies, will be presented in the conclusion section.

13.2 First Case Study: Ribeiriño Bridge (Ourense, Spain)

13.2.1 *Description and Building Materials of the Ribeiriño Bridge*

Located in Ourense county (northern Spain), Ribeiriño bridge (Fig. 13.2) is a key to the communication network between the cities of Santiago of Compostela and Madrid (capital and largest city of Spain). Predominantly built in reinforced and pre-stressed concrete (arc, abutments, bearings and piers) following the Spanish standard EH-68 (Ministerio de Fomento 1968). The construction entered in service in 1971.

Set in an environment with high level of humidity and under an average rainfall of 880 mm/yr, the bridge is 147 m long and it is supported by several piers along its structure. In the central span, these constructive elements are supported by a parabolic

Table 13.1 Technical specifications of the sensors used in the case studies.

		Trimble GX200	FARO Photon 80	Riegl LMS z390i
Active sensors	Measuring principle	Time of flight	Phase shift	Time of flight
	Wavelength	534 nm (green)	785 nm (VNIR)	1,550 nm (SWIR)
	Radiometric resolution	8 bits	11 bits	8 bits
	Deflection system	Oscillating flat mirror	Rotating mirror	Rotating mirror
	Field of view	360° H 60° V	360° H 320° V	360° H 80° V
	Standard deviation	1.4 mm for D $\leq$ 50 m	2 mm for D = 25 m	6 mm for D $\leq$ 50 m
	Range of measurement	2–350 m	0.60–76 m	1.50–400 m
	Angular resolution	Azimuth: 12″ Zenith: 14″	Azimuth and Zenith: 33″	Azimuth and Zenith: 3.6″
	Beam divergence	3 mm to 5 m	0.16 mrad	0.3 mrad
	Scan speed (p/s)	5,000	120,000	11,000
		Nikon D200	Nikon Coolpix L11	
Passive sensors	Camera type	Single-lens reflex camera	Compact digital camera	
	Sensor type	CCD	CCD	
	Sensor size	23.60 × 15.80 mm	5.76 × 4.29 mm	
	Pixels	2872 × 2592	2816 × 2112	
	Radiometric resolution	12 bits	8 bits	
	Focal length	18 mm	6.2 mm	
	Max aperture	3.5	2.8	

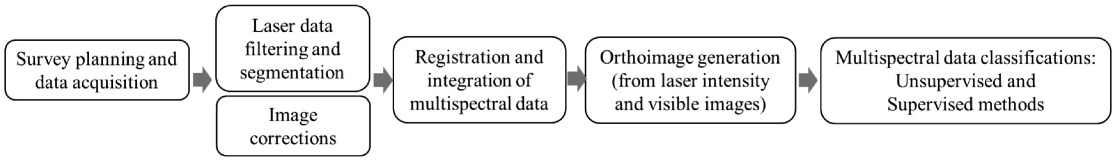

Figure 13.1 Workflow of the methodology proposed.

concrete arch. While the lateral spans (with a rectangular shape) are supported on several piers.

13.2.2 *Pathologies of the Structure*

Considering the environmental conditions previously defined: (i) High humidity on a cyclic basis; (ii) Concrete exposed to water contact; (iii) Presence of carbon dioxide; (iv) Possible attack of melting salts, the main pathological agent to be expected was the carbonatation corrosion. It can be also considered, to a lesser extent, to be chloride corrosion given the presence of a marine environment.

Although they have different origins, both corrosive processes, cause similar degrading result in concrete. For a better understanding, the concept of the steel passivation process should be reviewed.

Figure 13.2 Pier of the Ribeiriño bridge.

Passivation involves the formation of an inert film with a high pH (12.6–14) as a result of the hydration of Portland cement, in particular the calcium hydroxide component, forming the passive layer (physical protection against chemical aggressions).

Although this layer masks the steel against the action of external agents, the corrosion (presence of carbon dioxide and chloride) can promote the removal of this protective layer. As a consequence of its removal, a low pH environment is created and the steel is exposed to oxidation, causing a volume increase. This increase leads to the detachment of concrete areas and loss of mechanical adherence between steel and concrete. Complementarily, the presence of high levels of moisture, oxygen and a suitable temperature facilitates the growth of biological organisms on the bridge.

As a result of the different chemical attacks (mainly corrosion), the concrete durability is conditioned by the penetration of the several agents and the speed at which is attacked. Causing a decomposition of the elements and a loss of mechanical adherence between the steel and concrete.

To sum up two different pathologies will be expected:

- Biological colonization
- Moistures that can lead to corrosion by carbonation and chloride.

13.2.3 *Materials and Methods*

Considering the two pathologies mentioned above, it was decided to make a comparative multispectral study. To do this, we worked both with the radiometric results provided by the terrestrial laser scanner Riegl LMS z390i, in the SWIR range of the electromagnetic spectrum, and the photographs taken with a Nikon D200 camera built into the scanner (see Table 13.1).

The joint use of the laser scanner and the built in camera not only gives us an ideal 3D scene reconstruction. After a proper parallax-baseline correction, we can get a

true orthoimage with four multispectral channels (R, G, B and SWIR) increasing the spectral resolution of the study with the consequent enrichment in the pathological surveying of the bridge's pier.

The proposed methodology, which consists of several stages as shown in Figure 13.1, focuses on automation as a basic guideline to detect pathologies. Next, the procedures followed and its main characteristics are explained:

Planning and data acquisition. To carry out a proper data acquisition and to facilitate subsequent data process and orthoimage creation, the laser scanner was placed and leveled just once, 9 to 17 m far from the bridge. The spatial resolution achieved at this distance was 10 mm. Data acquisition was managed by Riscan Pro software, taking first data from laser intensity and then photographs in the selected area.

Filtering and segmentation. The first step of data processing consisted of point cloud filtering and segmentation of a selected area in which a great number of pathologies are presented, excluding all other irrelevant areas in the case study.

Data corrections. The separation of each RGB image in three different images (coming from red, green and blue channels), was performed through the free software DCRaw (Coffin 2011) by means of the Bayer demosaicing filter. As a result three images (1436 × 1296 pixels) were obtained.

Orthoimages generation. Once we have three separated images as mentioned above, and the SWIR one, coming from laser scanner, we obtained four orthoimages with Riscan Pro. Firstly, the orthoimage from the point cloud data, which incorporates intensity values in the SWIR range, was generated by the orthogonal projection of points in a plane parallel to the bridge structure. Then, to generate orthoimages in R, G and B channels the external camera orientation parameters with respect to the coordinate system of the laser model were obtained (registration). This step involves identifying and pointing out singular points in the images and the laser model. For this purpose we used external targets previously attached to the bridge. Finally, the projection of the points was performed using the collinearity condition (see Chapter 7). The final resolution of the orthoimages was 30 mm.

Multispectral data classification. The classification of these two groups (SWIR and SWIR+RGB) of orthoimages encloses a first *fuzzy k-means* unsupervised classification and a second *maximum likelihood* supervised classification:

- Unsupervised classification: the unsupervised classification algorithms based on the k-means approach is the most commonly used. It classifies a given data set in a certain number of clusters that are previously fixed. Within k-means algorithms, *fuzzy k-means* is one of the most frequently used. *Fuzzy k-means* give a specific weighting to each data associated with the inverse distance to the cluster's center.
- Supervised classification: the *maximum likelihood* classifier is the most complex, robust and reliable supervised algorithm, as it is closely based on the original data distribution. It considers that the radiometry (digital levels) of each category follows a normal distribution. It allows describing each category by a probability function from the mean vector and variance-covariance matrix. In this way, it is possible to calculate the probability that a given pixel belongs to a category.

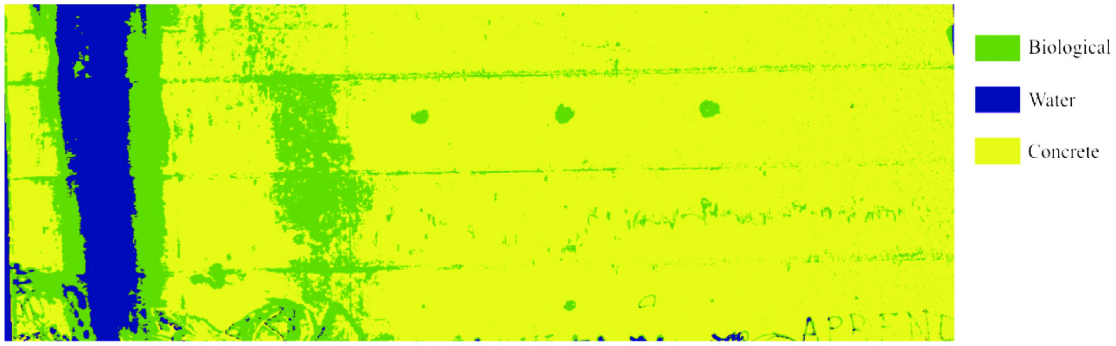

Figure 13.3 Supervised classification based on *fuzzy k-means* algorithm: SWIR (Laser) + RGB (Camera).

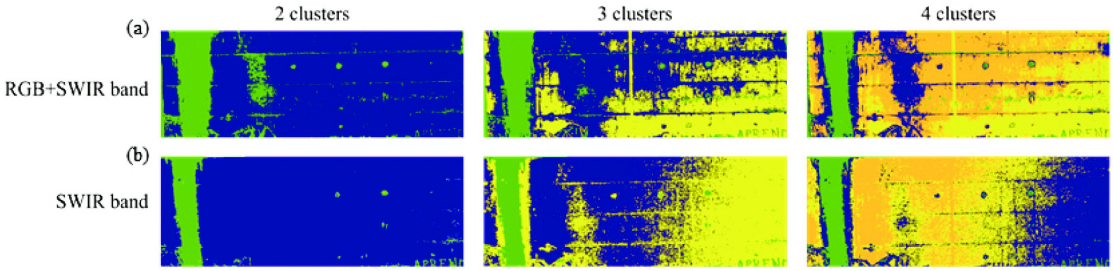

Figure 13.4 Unsupervised classification: (a) RGB + SWIR channels. (b) SWIR channel.

13.2.4 *Experimental Results*

At this point we must remember that the aim is to achieve an automatic process. This aim implies that the classification methodology should be a non-supervised classification one, which should be as close as possible to the ideal of a supervised process (which will act as a reference).

The supervised classification process, where user intervention to define training areas is required, was performed using the *maximum likelihood* algorithm (Fig. 13.3). For this purpose three informational classes were used, generating a Cohen's Kappa coefficient (Cohen 1968) of 0.97787.

The high value of Cohen's Kappa coefficient suggests good results in the classification process, but as seen in Figure 13.3, there are informational errors arising from classes not taken into account such as graffiti or drain pipes, where the presence of shadows generates several confusions. This fact reveals the limitations of the workflow based on the use of four channels, workflow applied in the discretization of informational classes that were not considered in the initial study.

Looking for the maximum possible automation, application of an unsupervised mono-channel classification (*fuzzy k-means*) (Fig. 13.4b) gives a biased result where clusters have no direct equivalence to informational classes (Fig. 13.3).

A four channels unsupervised *fuzzy k-means* classification (SWIR + RGB) gives better results (Fig. 13.4a). Using four clusters and applying an aggregation process to

guarantee the equivalence between clusters and informational classes, results are closer to the reality.

The quality assessment of the latest automated (non-supervised classification) results, contrasted with supervised process, shows an overall accuracy of 90.89%. The major errors come from the wrong assignment of concrete to biological class, and biological to water class. This second error has less effect because both classes represent aggressive pathologies for concrete, revealing the presence of moisture on it.

We can conclude that in a practical approach, when a general detection of pathologies is required, and the speed of data acquisition becomes important, a strategy based on the use of two sensors (active and passive) provides valid results in a completely automatic process. Moreover, from data acquired we can manage a metric 3D model of the construction.

13.3 Second Case Study: Santo Domingo Ruins (Pontevedra, Spain)

13.3.1 *Description and Building Materials of the Santo Domingo Ruins*

Popularly known as the "Ruins of Santo Domingo", which was once a Dominican monastery, is one of the most interesting historical-artistic properties of the Spanish north. The presence of tombs, heraldic shields and altarpieces rich in detail, unique and fragile, increases the value of the construction (Porto 1993). Built in granite, the beginning of its works dates from the first third of the XIV century. During its construction period, the monastery suffered different reforms, with the expansion of monastic stays. Nevertheless, the current building retains the main characteristics of the local Dominicans monasteries (Fig. 13.5).

Nowadays, the poor state of conservation of the different construction elements, together with the existence of biological colonization, loss of material, cracking and continuous leaks on the apses, expose this construction to a continued degradation process.

Figure 13.5 Santo Domingo ruins: (a) Front view of the façade. (b) Lateral view of the ruins.

The main construction material is the two-mica granite (at least in the area of the monastery ruins) (Montojo Santos et al. 2014). Such material was used to form the different masonry elements along the monastery. The different blocks were joined by lime mortar and complemented by underpinning rubbles.

For the artistic elements, the high level of biological colonization hinders the identification of the granite. It should be noted that the presence of accumulations of dark minerals (biotite and turmalita), with oxidation strips (iron oxide-hydroxides) gives a characteristic brown-rusty tone (Fig. 13.5).

13.3.2 *Pathologies of the Structure*

Subject to a wide variety of biological, atmospheric and structural degradation agents, the Santo Domingo ruins are an artistic-cultural property in an advanced state of degradation. Within the wide range of pathologies present in the building, the following degradation processes are expected to be detected:

- Efflorescence (white layer): given the presence of soluble salts, due to environmental conditions, mortars used in the restoration process, decorative materials employed in the different constructive elements or by capillary rise from the ground. This pathological effect starts with the crystallization of the salts, outside or into the material, causing a wedge effect (expansion) which degraded the material properties.
- Biological activity: materialized with the presence of moss, lichens, algae, plants with stem and remains of metabolic activity on the construction. This pathology causes a degradation of the mortar and rocks present on the different constructive elements (chemical erosion and fracture).
- Damp spots: on the pavement and walls, caused mostly by capillary rise. They are also visible on the ledges of the construction as a result of different runoffs.
- Crusts (black color): they appear throughout the building, their origin can be attributed to: (i) Biological colonization; and (ii) Contamination from urban activity. Both causes create dark color crusts with different grip levels on the affected area.

13.3.3 *Materials and Methods*

Although there are several tests capable of detecting damage, caused by different pathological agents, in the construction (e.g. X-ray diffraction, microscopes or chemical assays) (Montojo Santos et al. 2014), it is required to provide a quantification procedure, as was explained in the previous case study. Due to the characteristic of the construction, and the needed of a geometrical monitoring, the terrestrial laser scanner was the a priori best solution. Complementary to the geometrical data captured by this sensor, the radiometric information was employed, in order to carry out a multispectral image classification procedure.

Since the main goal of the present chapter is focused on the pathological detection by the radiometry captured by the different sensors used, the geometrical processing was omitted. For the present case study, and given the variety of pathologies presented, four sensors (three terrestrial laser scanners and a visible camera) were used. On the one hand, and in order to capture the visible spectrum, a time of flight

Trimble GX200 laser scanner (Green-534 nm) and a Nikon D200 digital camera were utilized. On the other hand and with the purpose of acquiring the near (NIR) and medium (SWIR) infrared spectrum, a FARO Photon (785 nm) and Riegl LMS z390i (1,550 nm) laser scanners were used (to see more about its technical specifications see Table 13.1).

As shown Figure 13.1, the methodology followed for the acquisition and evaluation of the results comprise a total of five stages, as explained below:

Planning and data acquisition. Prior to data collection, a visual inspection was performed to evaluate the different pathologies presented in the construction. Also it was to assess the accessibility and restrictions in the area. Additionally to the localization and the value of the construction, the environmental conditions were considered (e.g. high probability of rain and high humidity).

During the data acquisition process, the different laser scanners used were placed according to a plan previously prepared and at a distance from the façade between 5–10 m getting thirty one point clouds with a 10 mm of spatial resolution. This process was assisted by different software: Realworks Survey for Trimble, Scene 3D for Faro Photon 80 and Riscan Pro for Riegl LMS z390i. The number of scan stations was selected according to the different technical specifications provided by the manufacturer (Table 13.1).

Filtering and segmentation. Applied after data gathering, this stage comprises the filtering (denoising) and registration of the different point clouds. For the point clouds the alignment was considered the ICP (Iterative Closest Point) strategy.

Data corrections. Encloses the images demosaicking, since the camera used in this work utilizes a Bayer filter. For more details about this process consult the previous case study.

Orthoimages generation. For each point cloud registered, an orthoimage was generated providing a total of six channels: Four orthoimages in the visible range (R, G1, $G2_{Trimble}$ and B) and two in the infrared (NIR and SWIR) one. Taking the advantage of the registration performed in the previous step (with the different point clouds captured) the ortoimages were generated (see previous case study). As result 10 mm resolution images were obtained.

Multispectral data classification. The multispectral dataset, evaluated in the present case study, enclose a total of six orthoimages. A *fuzzy k-means* algorithm was used in the unsupervised classification (for more details see the previous case of study). Also a supervised classification was required with the aim of improving the results, by the addition of informational classes introduced by an expert.

13.3.4 *Experimental Results*

Starting from the geometrical base, provided by the orthoimage previously defined (with 10 mm of spatial resolution), the main goal now is the pathological clustering identification (in contrast to the material classification which is not considered). For this purpose an initial analysis (non-supervised) classification was carried out. Six informational classes were considered and a *fuzzy k-means* algorithm was used. The results of this process are shown in Figure 13.6, considering the following classes: (i) Granite without pathological affections; (ii) Pathologies arising from water (dampness) and

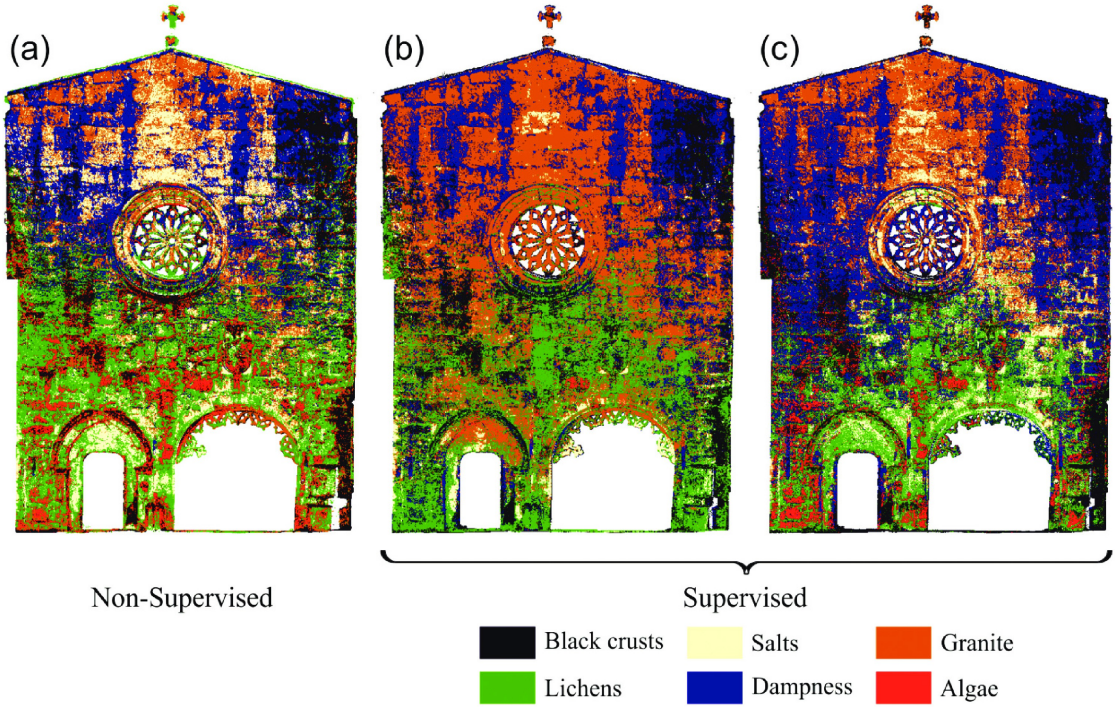

Figure 13.6 (a) Non supervised classification with merged classes. (b) Supervised classification with six channels. (c) Supervised classification with three channels (only active sensors).

salts; (iii) Two types of biological elements (lichens and algae); and (iv) Pathologies of decay (black crusts). Despite this initial study, the unsupervised classification, with six clusters and the employment of *fuzzy k-means* algorithm, fails to yield results close to real ones, even using all available channels.

Given the large variety of pathological processes presented in this construction, and some of them with similar origin (algae-lichen), the resulting analysis shows a radiometric overlap. Therefore it was required to increase the number of clusters to improve the separability between classes.

In order to enhance the unsupervised classification performance, it was necessary to establish an aggregation process (merge phase) attended by the user. The main goal of this process is to approximate the new clusters to the informational class showed in Figure 13.6a. This process is applied to the Biological colonization, moss and lichen classes, shown in Section 13.3.2.

Despite the aggregation process, classification results are far from optimal, with an overestimation of the affected areas by the pathological processes. The greatest variations were shown between biological agents. In view of the obvious errors occurring in the non-supervised process, it was necessary to use a supervised approach based on a *maximum likelihood* algorithm. Six classes, from the initial hypothesis and the six channels available, were considered in this classification process (Fig. 13.6b). Results (Table 13.2) show an overall accuracy of 0.8844 and a Cohen's Kappa coefficient of 0.8157 (excluding the null class).

Table 13.2 Supervised classification: confusion matrix with six channels.

	Black crusts	Lichens	Salts	Dampness	Granite	Algae
Black crusts	15.16%	0.18%	0.00%	1.73%	0.02%	0.02%
Lichens	0.02%	4.03%	0.02%	0.00%	0.02%	0.02%
Salts	0.00%	0.00%	1.44%	0.00%	0.02%	0.00%
Dampness	1.17%	0.25%	0.00%	17.29%	1.97%	0.04%
Granite	0.08%	1.52%	0.25%	4.17%	50.17%	0.06%
Algae	0.00%	0.00%	0.00%	0.00%	0.00%	0.35%

Table 13.3 Supervised classification: confusion matrix with five channels.

	Black crusts	Lichens	Salts	Dampness	Granite	Algae
Black crusts	15.01%	0.37%	0.00%	1.70%	0.00%	0.02%
Lichens	0.10%	3.98%	0.00%	0.02%	0.02%	0.02%
Salts	0.00%	0.02%	1.44%	0.00%	0.00%	0.00%
Dampness	1.13%	0.74%	0.00%	16.65%	2.18%	0.04%
Granite	0.14%	1.95%	0.31%	4.33%	49.41%	0.06%
Algae	0.00%	0.00%	0.00%	0.00%	0.00%	0.35%

Since the black crusts were associated to the granite decay caused by a granular disintegration due to the presence of dampness and/or soiling, there was a class overlap as shown in Table 13.3. In a similar way, the high level of deterioration of the façade (approx. half of it is affected by some kind of pathology) hindered the granite discretization for the different wavelengths.

Regarding the wavelengths and the overlap between green channels (Trimble GX200 and visible camera), the results provided by classifications carried out with five (excluding passive green channel) and six channels had a similar efficiency (Table 13.2 and Table 13.3).

Evaluating the statistical results, it is possible to observe a slight decline. The overall accuracy and Kappa coefficient go down to 0.8684 and 0.7916 respectively. This decline hardly has a negative effect on the final result, from a qualitative point of view. This change has its origin in the slight variations (during the classification) between lichens-dampness and lichens-granite classes. For the algae class any variation was observed given its spectral signature, with high variations in the visible zone (manifested through red/orange tonalities).

Classification results derived from the independent use of the active channels, three in total (Fig. 13.6c) corresponding with the different laser scanner used, seem to be insufficient. With an overall accuracy of 0.7526 and a Cohen's Kappa coefficient of 0.6367 (Table 13.4) this classification cannot be considered as the best one. It may lead to the wrong considerations for later restoration actions.

For these purposes, sensor hybridization was applied considering two classifications: (i) Five channels classification (three from the active sensors and two from the red and blue channel of the camera) and (ii) Six channels classification (adding to the previous channels clustering the green channel of the camera). As a result of this hybridization the classification improved (Table 13.2 and Table 13.3).

Table 13.4 Supervised classification: confusion matrix with three channels.

	Black crusts	Lichens	Salts	Dampness	Granite	Algae
Black crusts	14.92%	0.31%	0.00%	1.71%	0.00%	0.16%
Lichens	0.14%	2.84%	0.10%	0.02%	0.02%	0.97%
Salts	0.00%	0.27%	1.01%	0.00%	0.18%	0.00%
Dampness	0.95%	0.88%	0.08%	16.15%	2.32%	0.39%
Granite	0.08%	3.74%	6.55%	5.10%	40.02%	0.76%
Algae	0.00%	0.00%	0.00%	0.00%	0.00%	0.33%

Also there is a remarkable worsening in the unaffected material classification, since the granite used in this construction presents a heterogeneous texture, with large variations in the grain size and mineral distribution, requiring for instance an expansion in the number of channels used or the use of an additional algorithm based on spatio-contextual classification techniques (Li et al. 2014), in order to have an optimal result.

As shown in the results (Table 13.2 and Table 13.3), the addition of redundant channels, with overlapping (in terms of spectral signatures) areas, did not generate significant improvements. Regarding the use of channels from the cameras, despite having a bad radiometric resolution, they achieve better classification results in areas with several classes (that need to be classified), even without the presence of large pathologies on it.

13.4 Church of San Pedro Case Study (Avila, Spain)

13.4.1 *Description and Building Materials of the San Pedro Church*

The historical and cultural heritage of the city of Ávila is famous mainly due to its variety of medieval constructions both religious and civil in origin. Within this wide range of buildings the predominant use of granite masonry is certainly highlighted.

It is worth to noting that the construction material depended on its availability close to the working area. The presence of a granite deposit in the village of "La Colilla", just a few kilometers from the city, served as a quarry for the extraction of this construction material for buildings.

Much of the appeal of this heritage architecture lies in the wide variety of types of granites present in this quarry. A total of 5 granite varieties can be recognized and all of them have been used as building material in historical constructions in Ávila (Molina Ballesteros 1993): (i) Unaltered grey coarse-grained granite; (ii) Unaltered grey fine-grained granite; (iii) Ochre granite; (iv) Red granite and (v) White granite. Each of the three latter granite types is the result of several alterations produced during the Iberian Hercynian Base and presents its own physical and mechanical properties that were considered in the multispectral analysis.

The church of San Pedro is located in the old big market square devoted to Santa Teresa, facing the medieval door of the Alcazar, and is one of the most characteristic monuments of Romanesque architecture in the city. With a cross-shaped layout, it consists of three naves with five sections topped by three apses. It has a recognized dome base and a tower in the northern arm of the transept.

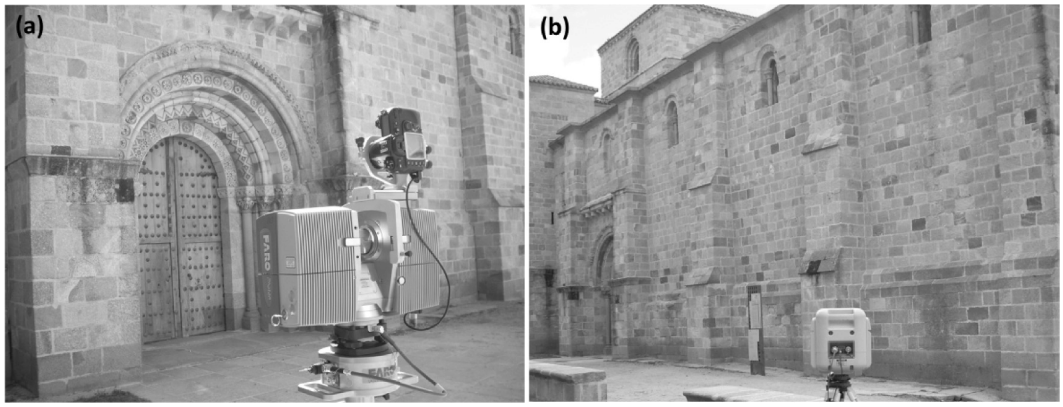

Figure 13.7 Church of San Pedro: (a) Detail view of the north entrance. (b) General view of the north façade (Flórez García, 2009).

Here, the different granite types of masonry combined on the façade are generally assessed (Fig. 13.7):

- The main façade (westward orientation): consists of a plinth and buttress of grey granite blocks. The use of this constructive solution in the upper archivolts and the pinnacles should be highlighted. The rest of the façade is built with ochre and red granite blocks.
- The eastern façade: consisting, similarly to the main façade, of a grey granite plinth (variable in height) and walls with ochre and red granite blocks.
- The north façade: slightly different from the rest, presents a red granite plinth and the rest of the elements are erected with ochre granite as predominant construction material.
- The southern façade: similarly to the western façade has a buttress fully erected in grey granite.
- The inside of the church: consists of a combination of ochre and grey granite. The grey granite was used for the pillars, since ochre granite was used for the rest of the structural elements (walls, arches, vaults, etc.).

13.4.2 *Pathologies of the Structure*

While white, ochre and red granites present better properties to be hewed and become part of the façade ornamentation: their physical-mechanical properties, such as water absorption, frost resistance, bending strength, shock and compression resistance, are worse than those of the grey granite from bedrock (García-Talegón et al. 1993). That is why a complete pathological evaluation with a comprehensive knowledge of the structure (finite element analysis, limit analysis, etc.) may yield not only a correct identification of the different construction materials but also detect possible pathologies of such materials as listed below:

- Grey granite: mainly composed of quartz, feldspar, mica and chlorite.
- Ochre granite: altered granite without chlorites, biotites and plagioclases. Its mineralogical composition consists of iron oxyhydroxides and phyllosilicates.

- Granite of reddish color: weathered granite that has undergone a kaolinization process with long periods of water saturation. It has a greater content of iron oxides.
- Degree of moisture: as a result of filtration and capillarity processes.
- Biological colonization: the effects of specific atmospheric conditions such as high humidity and temperature and the presence of oxygen lead to the proliferation and persistence of certain organisms on the rock.
- Color changes: as patinas of dirt, a damage due to environmental pollution.

13.4.3 *Materials and Methods*

In this case study, technologies such as terrestrial laser scanning and close range photogrammetry were again applied to analyze and diagnose the diseases presented in the different construction materials of the north façade of the church, because this façade is the most affected of the church.

A pathological assessment of the constructions was undertaken in response to the damage caused by external factors in the previous case studies. However, in this case the variability of different types of granites was examined as an intrinsic factor of the origin of pathologies. Thus it was decided to work in the visible and near infrared range to analyze the potential of these two spectral ranges in order to distinguish building materials. For the visible range and as an active sensor the laser scanner Trimble GX200 was used, whereas the compact camera Nikon Coolpix L11 was applied as passive sensor. For the near infrared range, the laser scanner FARO Photon 80 was selected (the technical characteristics of each sensor are listed in Table 13.1).

The methodology for the data analysis and the workflow followed are proposed in Figure 13.1: planning and data acquisition, filtering and segmentation, some data corrections, orthoimages generation and multispectral data classification.

Planning and data acquisition. An initial assessment and inspection of the area under study were essential to plan the multisensory data acquisition. Some possible limitations during data capture and the accessibility to the area depend on the time of day, number of stations and the distance established to the structure, among other factors. Therefore, the success in the fieldwork depends largely on the previous inspection. In this particular study various problems were observed: hidden areas caused by the projected shadows by two nearby buildings, inability to station the sensors in the desired position and frequent pedestrian traffic. Finally, the ideal moment was selected to achieve a homogeneous lighting to ensure uniformity in the radiometric values of the field campaign.

With laser scanners leveled properly, a total of 2 stations at a distance to the façade that varied between 6 and 3 m were performed. The final spatial resolution of the point cloud was 8 mm. As in previous cases, Trimble Realworks Survey and Scene 3D software were used for the data acquisition. Meanwhile, the Nikon Coolpix L11 was integrated into the FARO Photon 80 to take pictures simultaneously from the same point of view.

Filtering and segmentation. As has been mentioned, since the church was located in a city center and surrounded by some buildings, the multispectral study was very interrupted by pedestrian traffic and affected by the shadows projected by neighboring

buildings. Therefore, the first step of data processing was the segmentation of the point clouds leaving only data belonging to the façade of interest.

Data corrections. Some data required corrections such as carry out a proper registration and alignment of all stations belonging to each sensor. The targets disposed on the walls were used to perform the alignments, and therefore these targets should appear in each laser scan.

Orthoimages generation. After getting all the scans aligned and registered in the same coordinate system, the three orthoimages (from: RGB, $G_{Trimble}$, and NIR) were created. The orthoimage generation was carried out with the Trimble Realworks Survey software. Firstly, orthoimages from both laser scanners point clouds in the green and NIR ranges respectively were created and orthoimages from the RGB afterwards (similarly as in the previous case). The spatial resolution reached for the orthoimages was 20 mm.

Multispectral data classification. Finally, the set of three orthoimages arranged in a three-channels multispectral image was initially classified in an unsupervised way and subsequently in a supervised way. For the unsupervised classification the *fuzzy k-means* algorithm was used.

13.4.4 *Experimental Results*

The methodology required to ensure a right pathological classification of the structural materials involved performing a supervised classification. To this end, it was necessary to establish the suitable number of a priori informational classes and their connection with the data collected by all the sensors.

The initial hypothesis was set based on: (i) Three classes for construction materials (granites); (ii) Three classes for pathologies (two classes for moisture and one for biological factors); (iii) wood structures; and (iv) null class.

The study of mortar between blocks was not possible since its thickness was less than the GSD achieved with all sensors. This building material was perceptible only in the joints with a widest thickness of 3 cm while the spatial resolution of the orthoimages was 2 cm. Therefore, it was decided to dismiss it from the classification process.

Regarding the *fuzzy k-means* unsupervised classification, where the aforementioned hypothesis of clusters was established, provided results were not comparable even with the visual inspection. Therefore, it was necessary to fix other informational classes (a total of seven) including artificial elements of the guttering system, excluding wooden class present in the door and the union of the two types of unaltered granites in one class. This was necessary since the spectral resolution of the five-channels images generated was not enough.

The overall accuracy achieved in the classification shown in Figure 13.8 was 0.8835 with a Cohen's Kappa coefficient of 0.8328 for six informational classes (Table 13.5).

After the unsupervised classification by setting seven clusters, the roof gutters and metal rivets of the door were classified within the same class. Regarding the detection of pathologies on the façade, the confusion between moisture and biological factors should be noted (Table 13.6). This fact occurs because both pathologies are usually interrelated.

Moreover, the classes for which the worst value of separability (1.735/2.000) was obtained were "unaltered granite" and "penetrating damp", as shown in Table 13.6.

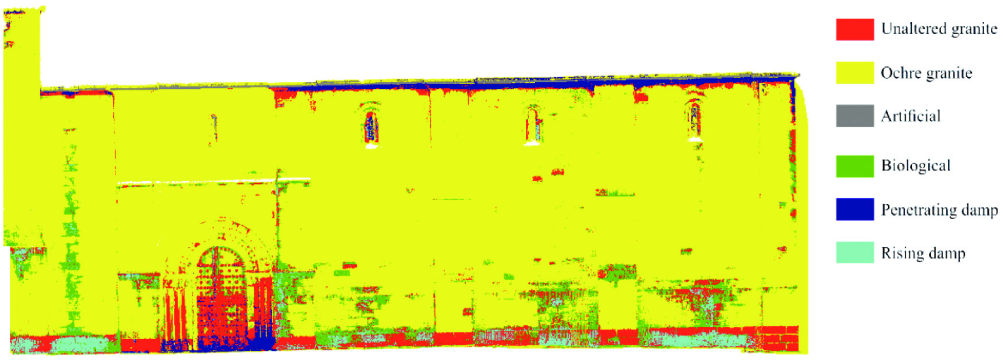

Figure 13.8 Orthoimage classification result after the supervised classification.

Table 13.5 Supervised classification: confusion matrix with six channels.

	Unaltered granite	Ochre granite	Artificial elements (e.g. gutter)	Biological colonization	Penetrating damp	Rising damp
Unaltered granite	82.28%	0.96%	0.00%	1.26%	15.48%	0.02%
Ochre granite	0.73%	98.70%	0.00%	0.57%	0.00%	0.00%
Artificial elements	0.00%	0.00%	100.00%	0.00%	0.00%	0.00%
Biological colonization	1.90%	1.33%	0.00%	84.30%	12.46%	0.00%
Penetrating damp	2.53%	0.00%	0.00%	6.41%	91.05%	0.00%
Rising damp	3.36%	0.00%	0.00%	0.00%	0.00%	96.64%

Table 13.6 Separability between classes.

	Unaltered granite	Ochre granite	Artificial elements	Biological colonization	Penetrating damp	Rising damp
Unaltered granite	–					
Ochre granite	1.99642	–				
Artificial elements	2.00000	2.00000	–			
Biological colonization	1.83363	1.98558	2.00000	–		
Penetrating damp	1.73514	2.00000	2.00000	1.87890	–	
Rising damp	1.98978	2.00000	2.00000	2.00000	1.99994	–

The main reason is the similar radiometric response of the unaltered granite and slightly damp unaltered granite and due to unaltered granite is only part of the façade plinth and this part of the structure is likely to be affected by rising damp.

As a general conclusion, it is important to highlight that limitations in robust discrimination potential of pathologies after the classification process is not only due to the radiometric resolution, which depends on the available sensors for each case study, but also depends on the smallest element that it is possible to discriminate, i.e. the spatial resolution of the orthoimages.

An approximate knowledge of the spectral signatures of the materials studied, although they come from laboratory tests, would help in the selection of the optimal wavelengths for the definition of effective informational classes.

13.5 Conclusions

Although the described methodology based on multispectral dataset management allows detecting and classifying accurately a variety of constructive pathologies, certain aspects such as peelings, cracks or disaggregation processes (abundant in masonry elements) are not completely explained. Given the flexibility of this methodology, which allows the analysis of data obtained by laser scanning and photogrammetry techniques, such degradation processes can be completely characterized through a geometric analysis of the construction. Also, the possibility of a large scale evaluation (large evaluated areas) and pathologies quantification are the strong points of photogrammetry and laser systems, making them valuable resources within the buildings' pathological assessment. However, as noted above, certain geometric aspects are not fully defined, as well as qualitative data on the material affected by pathological processes (which can be obtained by in-situ or laboratory test).

In order to make a full pathological assessment it is recommended to perform the following stages: (i) Geometric analysis (measuring deformations, settlements, kaolinization, etc.); (ii) Multispectral classification (using the described methodology); and (iii) Complementary qualitative in-situ and laboratory tests (use of reagents to assess biological colonization, mineralogical analysis, mechanical analysis, etc.).

Also essential is planning periodic field campaigns which will allow monitoring and assessing the pathological condition and the effectiveness of the applied restoration techniques.

Regarding the field campaigns, a series of particular best practices have been covered in the previous subsections. However, the optimal data acquisition protocol changes for the different spectral regions. When the discretization of the textural differences is required, the visible region is advisable, so the acquisition should be done with uniform light conditions. However, for a more detailed analysis of moisture (different degree of moisture) it is recommended to add a thermal infrared channel, which requires a light absence (mainly the solar effects) for an optimal data gathering. Although it is possible a priori knowledge of the material spectral signature, this information comes from laboratory test where not only the light conditions are controlled, but also specimens are optimal. In the field campaign, the constructive materials may have a heterogeneous appearance due to the textural differences which hinder their correct classification. In this regard, the use of additional SWIR channels, despite its worst geometric resolution, will improve their classification. Finally, the 3D spatial characterization of the study object is a strong point when the quantitative metric analysis associated to the areas affected is required. As additional advantage, the quantification of the prevention measures and their associated cost is directly drawn. When only a qualitative analysis is required, a pure 2D approach could be applied, supported by a projective transformation. However, the results and the resultant conclusions will be valid, only if the error budget is admissible and has been taken into account.

The current emergence of BIM (Building Information Modeling) and HBIM (Historical Building Information Modeling) multilayer models can be the perfect complement

to the methodology presented. As a result, it would be possible to create a complete information model including in it an exhaustive material characterization and pathological evaluation through time. As a result, analyses based on predictive models allow us to anticipate possible events, allowing to safeguard the integrity of the construction. It is in this field where the methodology presented could play a crucial role and provide added value.

References

Armesto-González, J., Riveiro-Rodríguez, B., González-Aguilera, D., & Rivas-Brea, M. T. (2010). Terrestrial laser scanning intensity data applied to damage detection for historical buildings. *Journal of Archaeological Science,* 37(12): 3037–3047. doi: http://dx.doi.org/10.1016/j.jas.2010.06.031.

Coffin, D. (2011). Raw digital photo decoding. Retrieved January 24, 2015.

Cohen, J. (1968). Weighted kappa: Nominal scale agreement provision for scaled disagreement or partial credit. *Psychological bulletin,* 70(4): 213.

Crespo, C., Armesto, J., González-Aguilera, D., & Arias, P. (2010). Damage Detection on Historical Buildings Using Unsupervised Classification Techniques. *ISPRS-International Archives of the Photogrammetry, Remote Sensing and Spatial Information Sciences, XXXVIII*, 184–188.

Del Pozo, S., Herrero-Pascual, J., Felipe-García, B., Hernández-López, D., Rodríguez-Gonzálvez, P., & González-Aguilera, D. (2015). Multi-Sensor Radiometric Study to Detect Pathologies in Historical Buildings. *ISPRS-International Archives of the Photogrammetry, Remote Sensing and Spatial Information Sciences, XL-5/W4*, 193–200.

Flórez García, E. (2009). *Aplicación de técnicas geomáticas al análisis y diagnóstico de patologías en edificios del patrimonio histórico*. Departamento de Ingeniería Cartográfica y del Terreno. Politécnica Superior de Ávila. Ávila.

García-Talegón, J., García del Amo, D., Iñigo, A., Menduiña, J., Molina Ballesteros, E., & Hernández, V. (1993). Propiedades físico mecánicas de los granitos empleados en la catedral de Avila procedentes del yacimiento de "La Colilla" (Avila).

González-Jorge, H., Gonzalez-Aguilera, D., Rodriguez-Gonzalvez, P., & Arias, P. (2012). Monitoring biological crusts in civil engineering structures using intensity data from terrestrial laser scanners. *Construction and Building Materials*, 31(0): 119–128. doi: http://dx.doi.org/10.1016/j.conbuildmat.2011.12.053.

Instrucción del Hormigón Estructural, E. (2008). EHE-08. *Madrid, Ministerio de Fomento, Secretaría General Técnica.*

Li, M., Zang, S., Zhang, B., Li, S., & Wu, C. (2014). A Review of Remote Sensing Image Classification Techniques: the Role of Spatio-contextual Information. *European Journal of Remote Sensing*, 47, 389–411.

Lu, W., & Tan, Y.-P. (2003). Color filter array demosaicking: new method and performance measures. *IEEE Transactions on Image Processing, 12*(10), 1194–1210.

Ministerio de Fomento (1968). Instrucción para el proyecto y ejecución del obras de hormigón en masa o armado. Madrid.

Molina Ballesteros, E. (1993). *Incidencia de las alteraciones del zocalo hercinico iberico en las caracteristicas de las rocas afectadas, empleadas como materiales de construccion. Los granitos de "La Colilla" (Ávila).* Paper presented at the Alteracion de granitos y rocas afines, empleados como materiales de construccion: deterioro de monumentos historicos. Actas del workshop, Consejo Superior de Investigaciones Cientificas, Avila, Spain, 1993.

Montojo Santos, C., López de Silanes Vázquez, M., Álvarez Andrés, J., Sánchez-Biezma Serrano, M. J., Prieto Lamas, B., Silva Hermo, B. M., & López Díaz, A. J. (2014). Las ruinas de Santo Domingo de Pontevedra.

Porto, C. M. (1993). Arte gótico en Galicia: los dominicos I.

Rodríguez-González, P., Pascual, J. H., Aguilera, D. G., Nieto, Á. L. M., Mancera-Taboada, J., Martín, N. S., & Hidalgo, M. Á. M. (2013). Aplicación de técnicas geomáticas al análisis y diagnóstico de patologías en el Patrimonio Arquitectónico. *Mapping* (161), 4–19.

Sánchez-Aparicio, L. J., Riveiro, B., González-Aguilera, D., & Ramos, L. F. (2014). The combination of geomatic approaches and operational modal analysis to improve calibration of finite element models: A case of study in Saint Torcato Church (Guimarães, Portugal). *Construction and Building Materials*, 70(0): 118–129. doi: http://dx.doi.org/10.1016/j.conbuildmat.2014.07.106.